COBEM 2023 27TH INTERNATIONAL CONGRESS OF MECHANICAL ENGINEERING

ABCM Brazilian Society of Mechanical Sciences and Engineering
27th ABCM International Congress of Mechanical Engineering
December 04-08, 2023, Florianópolis-SC, Brazil

COB-2023-2414
COMPARING CHARPY IMPACT TEST USING SPECIMENS OF DIFFERENT SIZES FOR AISI 4340 STEEL

Rodrigo Freitas Alvarenga
Guilherme Henrique Alves Andrade
Rafael Marques Borges Pacheco
João Pedro Cândido José
Sinésio Domingues Franco
Luciano José Arantes
Rosenda Valdés Arencibia
Federal University of Uberlândia, 2121, João Naves de Ávila Avenue, Campus Santa Mônica, Building 5F, Zip Code: 38400-902, Uberlândia, MG, Brazil. E-mail addresses: r.freitassa@gmail.com, eng.mec.guilhermeandrade@gmail.com, rafaelmbpacheco@gmail.com, joao.pcandido@hotmail.com, sdfranco@ufu.br, ljarantes@ufu.br, rosenda.arencibia@ufu.br.

Daniel Correia Freire Ferreira
Research and Development Center, Petrobras, Rio de Janeiro, Brazil.
E-mail address: danielcff@petrobras.com.br

Abstract. *This study aimed to compare the transition curve and the absorbed energy values obtained from testing Charpy specimens with different sizes. Specimens were made from AISI 4340 steel with two hardnesses (34 HRC and 40 HRC) and three sizes (10 × 10 mm², 5 × 10 mm² and 2.5 × 10 mm²). Subsequently, the absorbed energy values obtained from sub-size specimens were corrected following the ASTM A370-21. The results indicated that when comparing specimens with the same size, those with lower hardness present higher energy, due the higher level of material ductility. After correction, the dispersion associated with the DBTT values increased, leading to a worse result quality. The correction of the DBTT values using the ASTM A370 did not promote expressive changes on the DBTT values under the experimental conditions investigated. The exception was the specimen with a 2.5 × 10 mm² and 34 HRC for which, the difference between the DBTT values increased, indicating an accuracy loss. The ANOVA showed that, with the 95 % confidence level, the factor specimen size caused statistically significant effects on the USE values for 2.5 × 10 mm² and on LSE for 5 × 10 mm².*

Keywords: *Charpy impact test, ductile-to-brittle transition temperature, sub-size specimen, correction.*

1. INTRODUCTION

Charpy impact testing holds a significant position among the techniques used for determining the mechanical properties of materials and has found widespread application for this purpose. The test was first named after Georges Charpy, which has used a pendulum machine testing based on the design developed by S. Bent Russel in 1898. The pendulum machine was originally used for measuring the absorbed energy, but others parameter can be obtained (Manahan et al, 2008). Among the advantages of this technique, one can cite the ease of Charpy machine operation and short-duration tests. The properties obtained by this test are: ductile-to-brittle transition temperature (DBTT), absorbed energy (KV), shear fracture appearance (SFA) and lateral expansion (LE) (ASTM A370, 2021). Lucon (2016) also pointed out that the scientific community recognized that a more accurate understanding of the fracture behavior can only be possible using an instrumented Charpy test.

In some cases, there are certain components whose geometry does not allow evaluation using Charpy impact test in a standard size. For example, when the plate thickness is less than 10 mm, testing with full-size specimen is impossible. In these cases, testing must be based on sub-size or miniatured specimens (Wallin, 2020).

The ASTM A370 (ASTM, 2021) presents a table for correction of the absorbed energy values from Charpy tests conducted on sub-size specimens to full-size specimens. It is important to note that there are limitations regarding the correlation of KV obtained from specimens of different sizes. According to ASTM E23 (ASTM, 2023), establish a comprehensive correlation between them is unfeasible; however, limited correlations might be established for specific purposes based on specialized studies of specific materials and specimens.

Furthermore, in the scientific literature, only isolated comparisons were identified between outcomes from testing miniaturized and full-size specimens. Lucon et al. (2015a) conducted instrumented Charpy tests to characterize the impact properties of three steels utilized by NIST for creating Charpy reference specimens (4340 quenched and tempered with two energy levels, and T200 18Ni maraging steel). These tests were performed using different specimen size: full-size

(10 x 10 mm²), sub-size specimens of three types (3/4-size, 1/2-size and 1/4-size) and miniaturized Reduced Half-Size (RHS) for each steel. The authors concluded that to establish a correlation between them was partially challenging due to significant uncertainties in measured ductile-to-brittle transition temperatures (DBTT) and upper shelf energies.

Lucon et al. (2015b) established a correlation between DBTTs from Charpy impact tests performed on specimens of varying dimensions of line pipe steels. They concluded that the results exhibited strong agreement with literature-published findings. In turn, Wallin (2020) proposed a method for the conversion the absorbed energies of sub-size, reduced ligament and miniature sized Charpy-V specimens to full-size specimens. This conversion method can be used in temperatures between the shelves providing a single value conversion, in other words the ductile-to-brittle transition region.

Thus, the main objective of this study was to compare the transition curve and the absorbed energy values obtained during Charpy tests. For this purpose, specimens were made from AISI 4340 steel with two hardness levels (34 HRC and 40 HRC) and three different sizes (10 × 10 mm², 5 × 10 mm² and 2.5 × 10 mm²). Subsequently, the absorbed energy values obtained from sub-size specimens were corrected following the ASTM A370-21 (ASTM, 2021). Finally, ductile-to-brittle transition curves were plotted and DBTT values were determined for each case and compared.

2. METHODOLOGY

All specimens were manufactured from AISI 4340 steel, quenched and tempered at different temperatures to reach approximate hardness levels of 34 HRC and 40 HRC. For the Charpy impact tests, specimens of the following sizes were evaluated: full-size (10 × 10 × 55 mm³); and sub-size (5 × 10 × 55 mm³ and 2.5 × 10 × 55 mm³).

Full-size and sub-size specimens were manufactured following the ASTM A370 (ASTM, 2021) determination. In both cases, the specimens were extracted from cylindrical bars via electrical discharge machining (EDM), as shown in Figure 1. Subsequently, the specimen surfaces were ground using a Blanchard-type grinder, model RG-280 by the manufacturer S. A. Yadoya. The grinding process is necessary to satisfy macro and microgeometric tolerances that require a roughness Ra (arithmetic average roughness) less than 2 µm on notched surface and opposite face and 4 µm on other two surfaces.

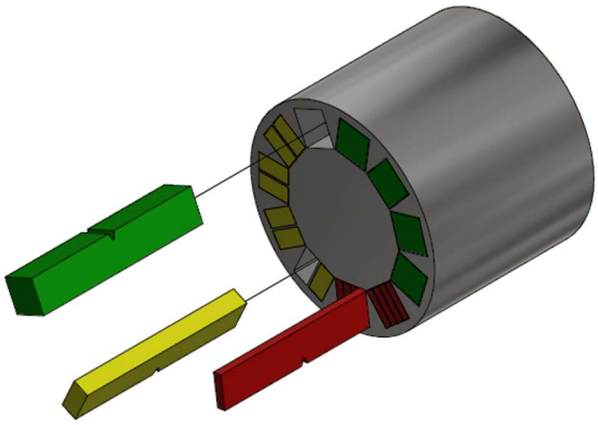

Figure 1. Scheme for removing specimens from the cylindrical bar made of AISI 4340 steel.

After the manufacturing process, the specimen quality control was performed. The depth, radius and notch angle were measured using an optical microscope (Olympus model BX51M, with a Carl Zeiss AxioCam ICc5 camera and the Carl Zeiss AxioVs40 V4.8.2 software). The thickness and width were measured using a digital external micrometer, with a resolution of 0.001 mm and a nominal range of 25 mm. The micrometer calibration certificate states an expanded uncertainty of 0.001 mm for a coverage factor (k) of 2.00. Three measurement cycles were conducted for all measurands.

All measurements were conducted at a controlled room temperature of 20.0 ± 1.0 °C. The room temperature was monitoring using a digital thermo-hygrometer, with a nominal range of -20.0 to 60.0 ºC and a 0.1 ºC resolution. The thermo-hygrometer calibration certificate states an expanded uncertainty of 0.3 ºC for a coverage factor (k) of 2.00. Before the measurements, the specimens, measuring systems, and measuring devices were left in the measurement room for 12 h to achieve thermal equilibrium.

Full-size and sub-size specimens were tested using a Charpy HIT 450P test machine from ZwickRoell equipped with a 8 mm radius instrumented striker. This machine had a nominal energy range of 450 J. To establish the ductile-to-brittle transition curve (full-size and sub-size specimens) different heating and cooling methods were used:

- Room temperature was 25 ± 1 ºC;
- For the range of -80 °C to 25 °C a thermal bath utilizing ethyl alcohol was employed, manufactured by Time Group Inc. under the model DWY-80A.

- For temperatures below -80 ºC, the specimen was submerged in liquid nitrogen and the heat exchange time was measured (using a thermocouple welded on a reference specimen) to achieve the desired temperature for the test using a reference specimen.
- Similarly, temperatures above room temperature were achieved by using an oil heating bath.

In tests carried out at temperatures from -80 ºC to 200 ºC, the transfer time between taking the specimen from the bath to the equipment and conducting the test did not exceed five seconds, as imposed by the ASTM E23 (2023). In addition, the tongs utilized for specimen transfer remained in contact during cooling and heating, to minimize thermal energy exchanges with the specimen.

Utilizing the absorbed energy values at distinct temperatures, the ductile-to-brittle transition curve was constructed employing the mathematical model of the asymmetric hyperbolic tangent (AHT) proposed by Wallin (2011), Eq. (1).

$$KV = \frac{USE + LSE}{2} + \frac{USE - LSE}{2} \cdot tanh\left(\frac{T - DBTT}{C + D \cdot T}\right) \tag{1}$$

In (1), *KV* is the absorbed energy (dependent variable); *T* is temperature (independent variable); *USE* (Upper Shelf Energy) is calculated as the average value of the energies obtained for shear fracture appearance (SFA) greater than 95 %. Specimens tested at temperatures greater than 83 ºC (150 ºF) above the Charpy upper-shelf onset were not considered, according to ASTM E185 (ASTM, 2021); *LSE* (Lower Shelf Energy) is calculated as the average value of the energies obtained for shear fracture appearance (SFA) less than 5 %; *DBTT* (ºC) is the Ductile-to-Brittle Transition Temperature. It corresponds to the abscissa of the point Y = (*LSE*+*USE*)/2; *C* (ºC) corresponds to the half-width of the transition region; and *D* determines how much the shape of the regression curve differs between lower and upper transition regions. In other words, the parameter *D* quantifies the asymmetry of the regression curve. If $D = 0$, the curve becomes symmetrical and coincides with hyperbolic tangent model (HT). If $D < 0$, the curvature in the lower transition region is larger than in the upper transition region; the opposite occurs when $D > 0$.

To facilitate comparisons, ductile-to-brittle transition curves were also plotted using corrected absorbed energy values according to ASTM A370-21 (ASTM, 2021). A statistical analysis was carried out by applying the Analysis of Variance (ANOVA) technique and through use of the software STATISTICA® to identify if the absorbed energy values obtained from sub-size specimens after correction and those provided by the tests using full-size specimens present difference between the means. For this purpose, two parameters (USE and LSE), two hardnesses (34 and 40 HRC), three sizes (10 × 10 × 55 mm³, 5 × 10 × 55 mm³ and 2.5 × 10 × 55 mm³) were considered.

3. RESULTS AND DISCUSSIONS

Figures 2 and 3 show the absorbed energy values as a function of testing temperature for the three examined specimen sizes. It is important to emphasize that these energy values have not yet been corrected in accordance with ASTM A370-21 (ASTM, 2021). In addition, these figures also show the ductile-to-brittle transition curves obtained via the AHT method.

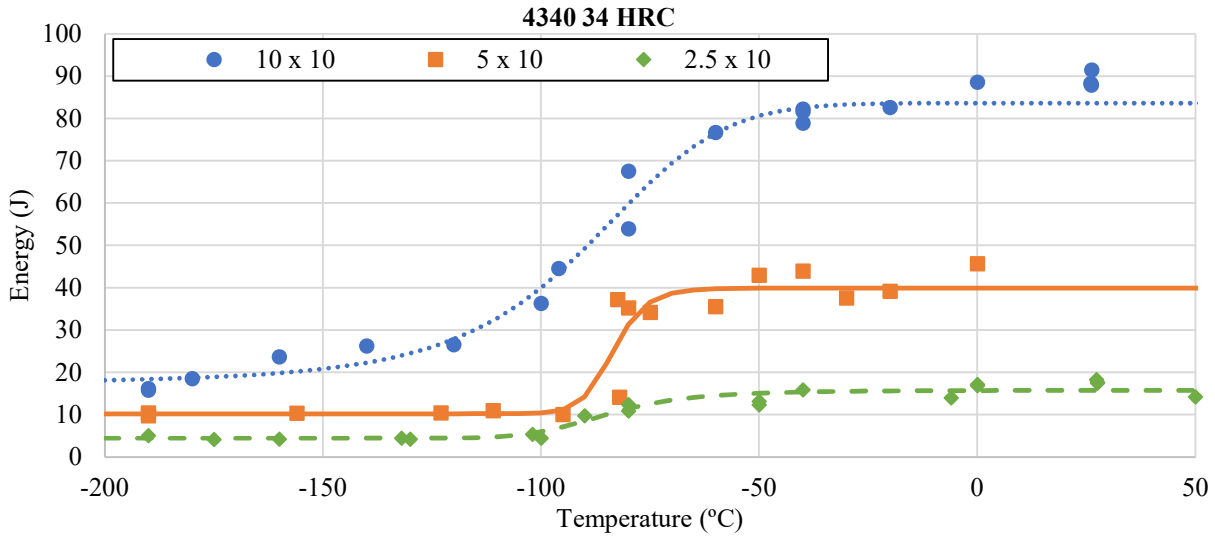

Figure 2. Ductile-to-brittle transition curves of AISI 4340 steel with hardness of 34 HRC.

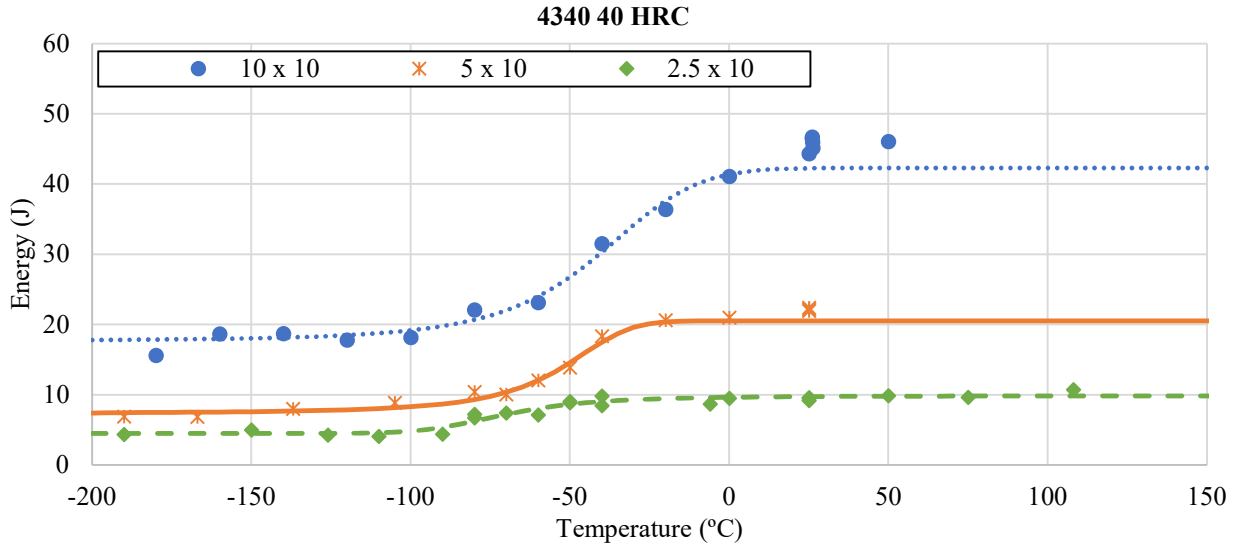

Figure 3. Ductile-to-brittle transition curves of AISI 4340 steel with hardness of 40 HRC.

From Figures 2 and 3, it can be concluded that the AHT method used to obtain the transition curves reveals a good fitting. The root mean square error (RMSE) was obtained for each curve. For these values to be comparable, they were divided by the energy value at the respective upper shelf energy (USE). For AISI 4340-34 HRC were 5.12 % for the 10 × 10 mm² size, 13.89 % for the 5 × 10 mm² and 9.86 % for the 2.5 × 10 mm². For AISI 4340-40 HRC steel, the respective RMSE/USE values were 6.23 % for the 10 × 10 mm² size, 5.17 % for the 5 × 10 mm² and 6.29 % for the 2.5 × 10 mm². The highest RMSE/USE value obtained for the curve of the material with a 34 HRC and size 5 × 10 mm² is justified by the greater dispersion associated with the absorbed energy values in the curve transition region. Moreover, as expected, it was observed that, for a given temperature, the absorbed energy exhibited a decreasing trend as the specimen cross-sectional area decreases. This fact can be justified since as the area is reduced, the lower the resistance that the specimen offers to the fracture.

Further analysis of Figures 2 and 3 show that when comparing specimens with the same sizes, those with lower hardness present higher energy. This fact suggests a higher level of ductility in this material. Lucon, McCowan and Santoyo (2015a) also observed that the material with the highest hardness yielded the lowest energy values within each region of the transition curve, while the opposite effect was observed in the case of the same material with lower hardness.

Figure 4a shows the standard uncertainty (u) associated with the absorbed energy values obtained at room temperature, considering three tests performed for each specimen size. Standard uncertainty values in percentage are shown in Figure 4b. It is important to note that the coverage probability was 68.27 %.

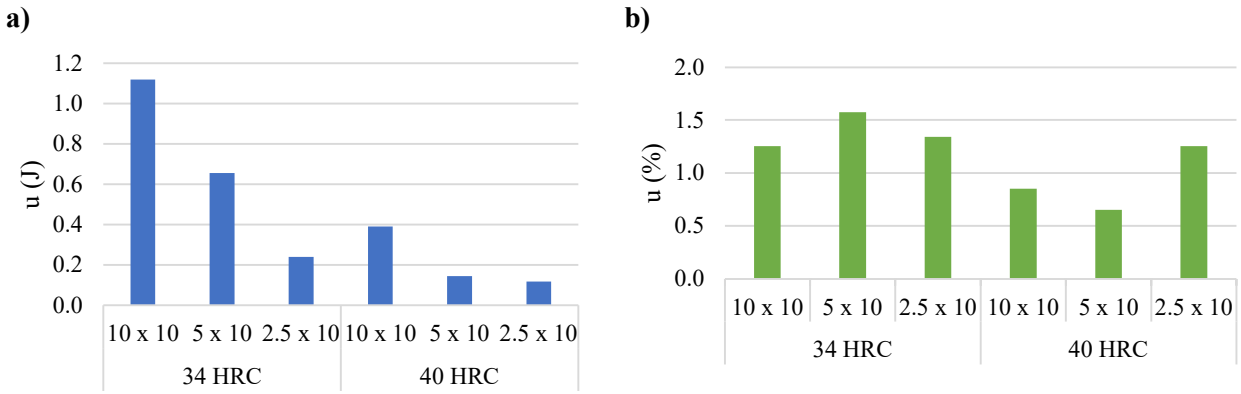

Figure 4.Standard uncertainty associated with absorbed energy values obtained at room temperature, considering three tests for each specimen sizes. a) in Joules and b) in percentage.

Noted in Figure4a was that the standard uncertainty associated with absorbed energy exhibits a clear decreasing trend as the specimen size increases. The highest uncertainty value, 1.1 J, was observed for specimens (10 × 10 mm² and 34 HRC). On the other hand, an opposite trend is observed in relation to material hardness, since lower uncertainty values

are obtained for materials with higher hardness. Figure 4b shows that the standard uncertainty represents less than 1.6 % in relation to average energy values, indicating a good result quality.

Figure 5 shows the ductile-to-brittle transition curves obtained by the AHT method for the corrected energy values (denoted by the letter "c") using ASTM A370 (2021) standard. For comparison purposes, the lower shelf energy (LSE) and upper shelf energy (USE) values extracted from Figs. 2, 3 and 5 are shown in Fig. 6.

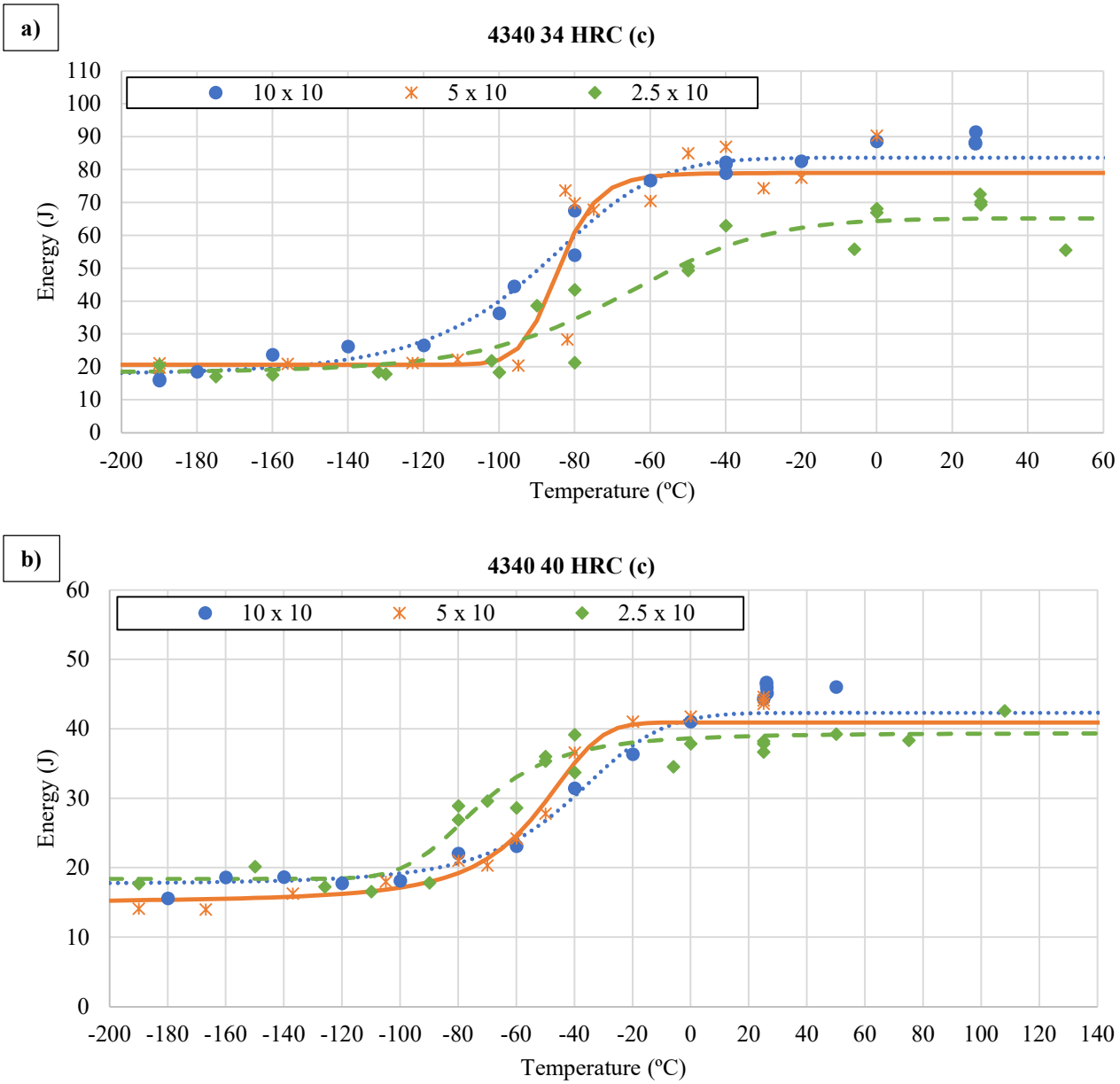

Figure 5. Ductile-to-brittle transition curves of the AISI 4340 steel specimens with energies corrected according to Table 9 of the ASTM A370-21 standard (ASTM, 2021) with hardness of (a) 34 HRC and (b) 40 HRC.

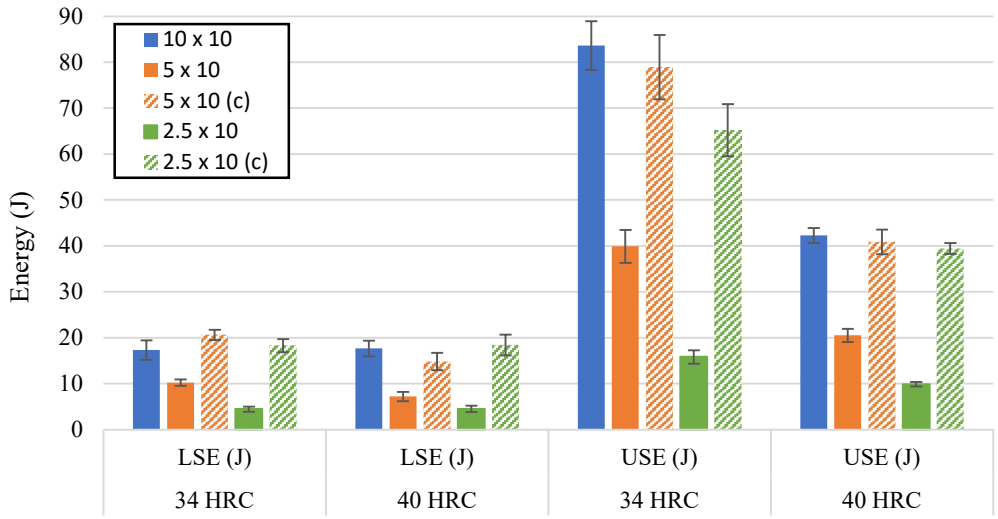

Figure 6. LSE and USE values obtained in Charpy tests of full and sub-size specimens and the conversion of values from the corrections of the ASTM A370 standard (ASTM, 2021).

After correction, the RMSE/USE values for AISI 4340- 34 HRC were 13.82 % for the 5 × 10 mm² and 10.12 % for 2.5 × 10 mm². In turn, for AISI 4340-40 HRC, the respective RMSE/USE values were 5.19 % for the 5 × 10 mm² and 6.33 % for the 2.5 × 10 mm². These values were statistically unchanged by the correction.

Figures 5 and 6 suggest that, for both levels of hardness, the corrected LSE values were higher than those obtained from full-size specimens except for 40 HRC and cross-section of 5 × 10 mm². For 34 HRC, percentage differences of 19.3 % and 5.8 % were noted, while for 40 HRC, these values were 16.0 % and 4.2 %, respectively, for specimens with thicknesses of 5.0 and 2.5 mm. Furthermore, the corrected USE values are lower than those obtained from tests using full-size specimens. In the case of the 34 HRC, percentage differences of 5.6 % and 22.0 % were observed, and for the 40 HRC, these percentages were 3.3 % and 6.7 %, respectively, for specimens with thicknesses of 5.0 and 2.5 mm.

The results (p-value) obtained by the analysis of variance (ANOVA) are shown on Table 1.

Table 1. ANOVA results for absorbed energy values obtained from different sub-size specimens after correction and that provided by the tests using full-size specimens.

	Hardness (HRC)	**5 × 10 mm²**	**2.5 × 10 mm²**
USE	34	0.074	5.53E-06
	40	0.280	0.008
LSE	34	0.017	0.214
	40	0.020	0.536

From Table 1, the conclusion reached is that, with the 95 % confidence level, the factor specimen size caused statistically significant effects on the USE values for 2.5 × 10 mm² and on LSE for 5 × 10 mm². By contrast, this factor did not cause statistically significant effect on USE for 5 × 10 mm² and on LSE for 2.5 × 10 mm². The normal probability plot of the residuals indicated that the residuals have a near normal distribution for the all investigated conditions.

Figure 7 shows the DBTT values obtained before and after correction. The standard uncertainty associated with transition temperatures (before correction) using different specimen sizes was 4.2 ºC for AISI 34 HRC and 8.4 ºC for AISI 40 HRC. After correction, these values were 7.0 ºC and 8.6 ºC, respectively. This fact indicates that after the ASTM A370 correction the dispersion associated with the DBTT values increased, leading to a worse result quality.

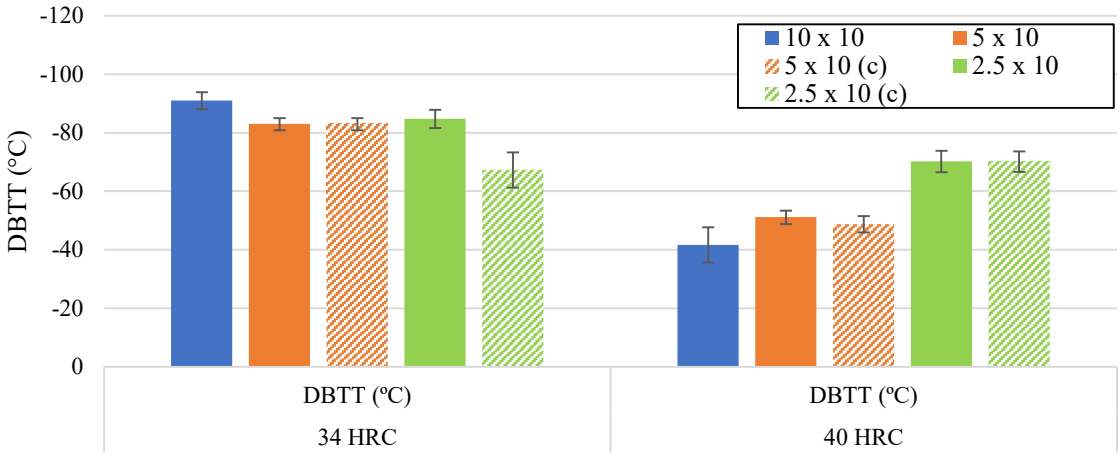

Figure 7. Values of ductile to brittle transition temperature measured from specimens of different sizes and hardness before and after ASTM A370 correction.

In addition, from Figure 7 it was observed a decreasing trend towards the DBTT values for 40 HRC as the fracture area decreases. By contrast, for 34 HRC, the DBTT values were higher in the sub-size specimen when compared to full-size. This behavior has also been observed by Lucon et al., (2015a). It is also noted that the DBTT correction using the ASTM A370 (ASTM, 2021) did not promote a significant change on the DBTT values under the experimental conditions investigated, with the exception of the specimen with a 2.5 × 10 mm^2 and 34 HRC. In this case, the difference between the DBTT values increased, indicating an accuracy loss.

4. CONCLUSIONS

When comparing specimens with the same dimension, those with lower hardness present higher energy. This fact suggests a higher level of ductility in this material.

The AHT method used to obtain the transition curves reveals a good fitting. After correction, the RMSE/USE values for AISI 4340- 34 HRC were 13.82 % for the 5 × 10 mm² and 10.12 % for 2.5 × 10 mm². In turn, for AISI 4340-40 HRC, the respective RMSE/USE values were 5.19 % for the 5 × 10 mm² and 6.33 % for the 2.5 × 10 mm². These values were statistically unchanged by the correction.

The standard uncertainty associated with transition temperatures (before correction) using different specimen sizes was 4.2 ºC for AISI 34 HRC and 8.4 ºC for AISI 40 HRC. After correction, these values were 7.0 ºC and 8.6 ºC, respectively. This fact indicates that after the correction the dispersion associated with the DBTT values increased, leading to a worse result quality.

A decreasing trend towards the DBTT values for 40 HRC was observed as the fracture area decreases. By contrast, for 34 HRC, the DBTT values were higher in the sub-size specimen when compared to full-size.

The correction of the DBTT values using the ASTM A370 (ASTM, 2021) did not promote an expressive change on the DBTT values under the experimental conditions investigated, with the exception of the specimen with a 2.5 × 10 mm^2 and 34 HRC. In this case, the difference between the DBTT values increased, indicating an accuracy loss.

The ANOVA showed that, with the 95 % confidence level, the factor specimen size caused statistically significant effects on the USE values for 2.5 × 10 mm^2 and on LSE for 5 × 10 mm^2.

Further tests must be carried out for a better definition of the absorbed energy values in the transition regions of the full-size and sub-size specimens.

5. ACKNOWLEDGEMENTS

The authors would like to thank Petrobras and the Brazilian financing agencies *Coordenação de Aperfeiçoamento de Pessoal de Nível Superior* (CAPES) and *Fundação de Amparo à Pesquisa do Estado de Minas Gerais* (FAPEMIG) for supporting the development of this research.

6. REFERENCES

ASTM A370-21, 2021. Standard Test Methods and Definitions for Mechanical Testing of Steel Products, ASTM Book of Standards 11.01, 2021.

ASTM E185, 2021. Standard Practice for Design of Surveillance Programs for Light-Water Moderated Nuclear Power Reactor Vessels, ASTM Book of Standards 09.01, 2021.

ISO 14556, 2015. Steel – Charpy V-notch pendulum impact test – Instrumented test method, International Standards Organization, 2015.

Lucon, E., McCowan, C.N. and Santoyo, R.L., 2015a, Impact Characterization of 4340 and T200 Steels by Means of Standard, Sub-Size and Miniaturized Charpy Specimens, NIST Technical Note 1858, February 2015.

Lucon, E., McCowan, C.N. and Santoyo, R.L., 2015b, Impact Characterization of Line Pipe Steels by Means of Standard, Sub-Size and Miniaturized Charpy Specimens, NIST Technical Note 1865, February 2015.

Lucon, E., 2016. Estimating dynamic ultimate tensile strength from instrumented Charpy data. Materials and Design, Vol. 97, p 437-443.

Manahan Jr, M.P., McCowan, C.N. and Manahan Sr, M.P., 2008. Percent Shear Area Determination in Charpy Impact Testing. Journal of ASTM International, Vol. 11, No 7.

Wallin, K, 2011. Fracture Toughness of Engineering Materials: Estimation and Application. EMAS Publishing, Warrington, GBR.

Wallin, K, 2020. Sub-sized and miniature CVN specimen conversion methodology. International Journal of Pressure Vessels and Piping. Vol. 183, pp. 104080.

7. RESPONSIBILITY NOTICE

The authors are the only responsible for the printed material included in this paper.